CRYSTAL GROWTH & DESIGN

Article

Cite This: Cryst. Growth Des. XXXX, XXX, XXX-XXX

pubs.acs.org/crystal

Highly Interpenetrated Robust Microporous Hydrogen-Bonded Organic Framework for Gas Separation

Wei Yang,[†] Jiawei Wang,[‡] Hailong Wang,*[,†] Zongbi Bao,[†,‡] John Cong-Gui Zhao,[†] and Banglin Chen*[,†]

[†]Department of Chemistry, University of Texas at San Antonio, San Antonio, Texas 78249-0698, United States

[‡]Key Laboratory of Biomass Chemical Engineering of Ministry of Education, College of Chemical and Biological Engineering, Zhejiang University, Hangzhou 310027, P. R. China

Supporting Information

ABSTRACT: A hydrogen-bonded organic framework (HOF), HOF-11, has been successfully prepared by the slow diffusion of hexane into a tetrahydrofuran solution of tris(4-carboxyphenyl)amine (TCPA). HOF-11 has been characterized by single-crystal and powder X-ray diffraction analysis, which is composed of TCPA ligands connected by the intermolecular hydrogen-bonding interactions in the carboxylic group dimer, showing 11-fold interpenetrated three-dimensional hydrogen-bonded networks in a (10,3)-b topology with the pore size of 6.2 × 6.8 Å^2. The permanent porosity of degassed HOF was demonstrated by virtue of the CO_2 sorption and selective gas adsorption.

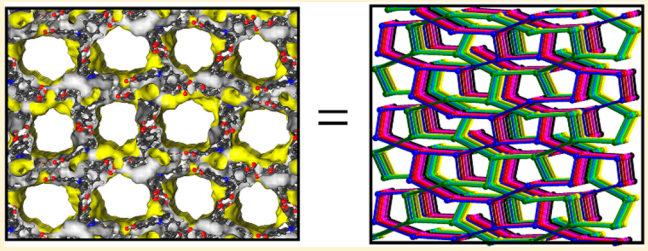

INTRODUCTION

Since the discovery of the hydrogen-bonded Dianin's compound as an organic zeolite in 1976,[1] continuous efforts in the fields of crystal engineering and materials chemistry have been devoted to the design and synthesis of porous molecular materials with desired properties on the platform of exquisite understanding and exploitation of intermodular interactions.[2−9] Hydrogen-bonded organic frameworks (HOFs) gradually emerge as a new family of porous molecular and crystalline materials,[10−12] attributed to their multiple directional hydrogen bonds which can sustain the porous HOF structures. As illustrated in a number of HOFs since 2010,[11−14] the combination of suitable organic skeletons and hydrogen-bond moieties has generated a variety of functional HOFs with potential applications in gas/molecule adsorption,[13−21] separation,[22−29] sensing,[30] semiconductor,[31] and proton conduction.[32,33] Among various organic skeletons, those C_3-symmetric skeletons,[23−26,32,34−39] mainly 1,3,5-substituted benzene derivatives, are the most popular and prone to form various stable (6,3) honeycomb-shaped supramolecular nets with the help of hydrogen-bonding synthons, which therefore have been comprehensively explored to construct HOFs. These two-dimensional (2D) hydrogen-bonded honeycomb-shaped networks are either directly packed via intermolecular $\pi-\pi$ interactions or interpenetrated with each other to provide permanent voids. Nevertheless, the three-dimensional (3D) hydrogen-bonded robust porous network assembled from C_3-symmetric building blocks have been rarely reported thus far, to the best of our knowledge.

Given the fact that the crystallization, an assembly process to reticulate building block into porous HOFs, is driven by the force of self-recognition and molecular aggregation, remarkable insights have been gain in the promotion of the hydrogen-bonding interaction between building blocks and the preclusion of the solvent participation in the framework. In this regard, the carboxylate···carboxylate dimer synthon constitutes a classic example of hydrogen-bonding moieties in the self-assembly of discrete molecules into HOFs.[16,36,39−41] With these in mind, triphenylamine (TPA) has been chosen to decorate with carboxylate groups to provide a new C_3-symmetric module, and the variation, from an sp^2 hybridization core for the benzene ring in 1,3,5-substituted benzene derivatives to an sp^3 hybridization center of nitrogen atom in TPA, is expected to afford new functional HOFs. Herein, we report a robust microporous 3D HOF, (HOF-11), which is composed of tris(4-carboxyphenyl)amine (TCPA) ligands linked via the intermolecular hydrogen-bonding interactions in carboxylate··· carboxylate dimers (Scheme 1). The crystal structure shows that HOF-11 is made up of 11-fold interpenetrated networks in a (10,3)-b topology. The 3D hydrogen-bonded structure exhibits 1D channels with the pore size of ∼6.2 × 6.8 Å^2. The desolvated framework manifests permanent porosity and selective adsorption of C_2H_2 and CO_2 over CH_4 and N_2.

EXPERIMENTAL SECTION

General Remarks. All chemicals were employed directly as received from the companies without further treatment. The precursors, tris(4-bromophenyl)amine and tris(4-cyanophenyl)amine, were synthesized referring to the reported procedures (Scheme 2).[29,42] During the preparation of this manuscript, the TCPA ligand was

Received: September 18, 2017
Revised: October 11, 2017

© XXXX American Chemical Society

DOI: 10.1021/acs.cgd.7b01322
Cryst. Growth Des. XXXX, XXX, XXX−XXX

Scheme 1. Schematic Molecular Structures of Building Blocks of TCPB and TCPA[a] together with Hydrogen-Bonded Organic Framework Topologies

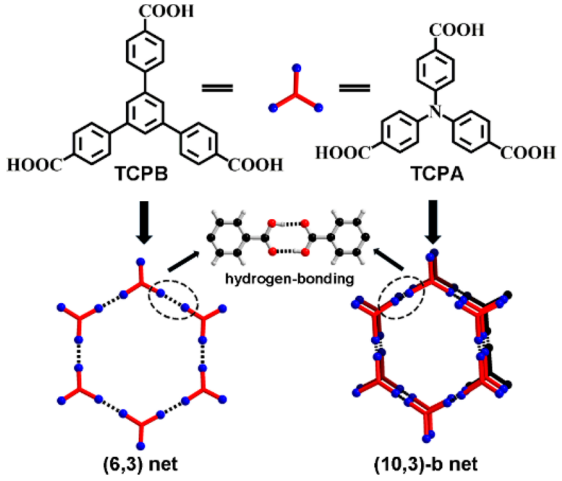

[a]TCPB = 1,3,5-tris(4-carboxyphenyl)benzene and TCPA = tris(4-carboxyphenyl)amine).

reported to assemble an isostructural HOF but in an absolutely different crystallization method.[43] The corresponding topological structure was not investigated, and the gas behaviors were completely different, possibly due to the different guest molecules influencing the activation process and thus the gas sorption.

Synthesis of Tris(4-bromophenyl)amine. To a 100 mL flask containing triphenylamine (2.5 g, 10.0 mmol) in 40 mL dichloromethane bathed in the ice–water, liquid bromine (1.6 mL, 31.5 mmol) was slowly added over 30 min. The resulting reaction mixture was further stirred for additional 48 h at room temperature. Then, the CH_2Cl_2 was evaporated and suspended in 100 mL of ethanol/water (v:v = 1:9). The precipitate was filtered and washed by water. The yield of tris(4-bromophenyl)amine was 4.3 g (89%). The product was used directly without further purification. ^{1}H NMR ($CDCl_3$, 500 MHz) δ (ppm): 7.39 (d, 6H) and 6.96 (d, 6H).

Synthesis of Tris(4-cyanophenyl)amine. Tris(4-bromophenyl)-amine (4.0 g, 8.3 mmol), CuCN (3.0 g, 33.3 mmol), and dimethylformamide (30 mL) were placed in a 100 mL Schlenk flask. The mixture was refluxed for 48 h under nitrogen atmosphere, and then suspended into 150 mL water. Ethylenediamine (5 mL) was added, and the resulting mixture was stirred at 100 °C for 1 h and filtered. The precipitate was extracted with dichloromethane (3 × 50 mL). The combined organic phase was dried with $MgSO_4$, filtered, and evaporated in a vacuum. The residue was repeatedly purified by chromatography on silica using a hexane/CH_2Cl_2 (1:1) as eluent, giving tris(4-cyanophenyl)amine 1.5 g with a yield of 55%. ^{1}H NMR ($CDCl_3$, 500 MHz) δ (ppm): 7.62 (d, 6H) and 7.17 (d, 6H).

Synthesis of Tris(4-carboxyphenyl)amine (TCPA). A mixture of tris(4-cyanophenyl)amine (2.0 g, 6.2 mmol) and NaOH (1.2 g, 30 mmol) in water (40 mL) was stirred and refluxed for 24 h under nitrogen atmosphere. After the resulting mixture was cooled to room temperature, the pH value of solution was adjusted to 5–6. The solid was filtered and washed with water, then dried under a vacuum at 50 °C to give a white solid (2.2 g) with a yield of 95%. ^{1}H NMR (DMSO-d_6, 500 MHz) δ (ppm): 12.80 (s, 3H), 7.92 (d, 6H), and 7.15 (d, 6H). It was found that 300 mg TCPA was able to be completely dissolved in 6 mL of THF in the solubility test, and the solubility of TCPA in THF therefore is about 50 mg/mL. Colorless crystals of HOF-11 were obtained by allowing hexane to slowly diffuse into a tetrahydrofuran (15 mL) solution containing TCPA (200 mg). After about 10 days, the HOF-11 single crystals were collected, which were washed using hexane for the further use. HOF-11a crystals were selected from the bulk material of degassed HOF-11.

Physical Measurements. NMR spectra were collected on a Varian INOVA 500 MHz spectrometer at room temperature. The internal standard of δ = 7.26 ppm and δ = 2.50 ppm was employed in ^{1}H NMR spectra collected in $CDCl_3$ and DMSO-d_6 solution, respectively. Thermogravimetric analysis (TGA) was performed on a Shimadzu TGA-50 thermogravimetric analyzer under N_2 atmosphere with a heating rate of 3 °C/min. Powder X-ray diffraction (PXRD) data were recorded on a Rigaku Ultima IV diffractometer. As-obtained crystals of HOF-11 were directly degassed for 24 h to 6 μmmHg at room temperature to provide activated phase (HOF-11a). Various gas sorption isotherms of HOF-11a were recorded on a Micromeritics ASAP 2020 surface area analyzer, and the measurement temperature was maintained at 196 K with a dry ice-acetone slurry, 273 K with an ice–water bath, and 296 K with a water bath in an air-conditioned 23 °C laboratory.

Crystallographic Investigation. Crystallographic data of HOF-11 and HOF-11a single crystals were recorded on an Oxford Diffraction SuperNova diffractometer with Cu Kα radiation (λ = 1.54184 Å). The crystal structures were solved based on the direct method (SHELXS-97) and refined on the foundation of full-matrix least-squares (SHELXL-97) on F^2.[44] Furthermore, we note that the "SQUEEZE" program was run to remove the disordered guest molecules in the HOF channels.[45] Selected crystallographic data and refinement parameters for these two species are summarized in Table 1, and hydrogen-bonding geometries used for the construction of HOFs are shown in Table 2. CCDC 1573633 and 1573634 for HOF-11 and HOF-11a crystal, respectively, contains the supplementary crystallographic data for this paper. These data can be acquired free of charge from the Cambridge Crystallographic Data Centre via www.ccdc.cam.ac.uk/data_request/cif.

IAST Calculation. The fitting of single-component C_2H_2, CO_2, CH_4, and N_2 adsorption isotherms was carried out according to the dual-site Langmuir–Freundlich (DSLF) model to aquire the useful parameters for the ideal adsorbed solution theory (IAST) calculation.[46,47] The theoretical adsorption isotherms and gas selectivities of mixed C_2H_2/CH_4 (50:50), CO_2/CH_4 (50:50), and CO_2/N_2 (10:90) at 273 and 296 K, respectively, were determined based on the IAST method.[48]

RESULTS AND DISCUSSION

Synthesis of Tris(4-carboxyphenyl)amine and HOF-11. The bromination reaction between triphenylamine and Br_2 in a dichloromethane solution yielded tris(4-bromophenyl)-amine. Then, tris(4-cyanophenyl)amine was prepared by the reaction of tris(4-bromophenyl)amine and CuCN in the DMF, which was further hydrolyzed in the presence of NaOH and acidized using HCl to afford tris(4-carboxyphenyl)amine. The excellent solubility (~50 mg/mL) of TCPA in THF is a very useful physicochemical property to assemble robust HOFs, because, on the experimental aspect, the exploitation of solvent

Scheme 2. Schematic Synthesis of the Module (TCPA) for the Self-Assembly of HOF-11

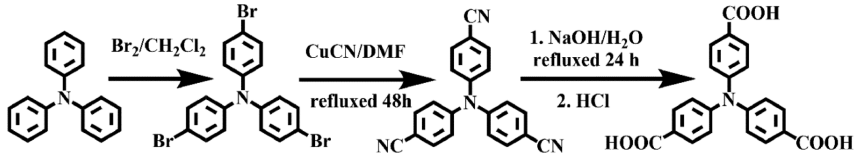

DOI: 10.1021/acs.cgd.7b01322
Cryst. Growth Des. XXXX, XXX, XXX–XXX

Table 1. Crystallographic and Refinement Parameters for HOF-11 and HOF-11a

crystal data	HOF-11	HOF-11a
system	monoclinic	monoclinic
space group	$P2_1/n$	$P2_1/n$
MF[a]	$C_{21}H_{15}NO_6$	$C_{21}H_{15}NO_6$
FW[a]	377.34	377.34
a /Å	7.3337(6)	7.3200(4)
b /Å	26.482(2)	26.982(3)
c /Å	49.894(4)	49.968(4)
α/deg	90	90
β/deg	92.622(2)	92.692(5)
γ/deg	90	90
volume/Å^3	9679.9(14)	9858.2(15)
Z	16	16
density/g/cm^3	1.036	1.017
solvent-accessible[4] void space /%	33.2	33.7
theoretical pore volume/cm^3/g	0.32[b]	0.33[a]
refinement	R_1 = 0.0721[c]	R_1 = 0.0947[c]
parameters	wR_2 = 0.2098[d]	wR_2 = 0.2629[d]
CCDC no.	1573633	1573634

[a]Molecular formula (MF) and formula weight (FW) were calculated based on the crystal structures without the consideration of guest molecules. [b]Calculation based on the HOF crystal structures using PLATON software.[43] [c]$R_1 = \Sigma||F_0|-|F_c||/\Sigma|F_0|$; [d]$wR_2 = [\Sigma w(F_0^2-F_c^2)^2/\Sigma w(F_0^2)^2]^{1/2}$.

with medium polarity (such as dichloromethane, acetone, and tetrahydrofuran) seems to be able to effectively preclude the solvent-participation in the construction of porous framework and only to be filled the voids of HOFs as guest molecules.[16,29,36] Colorless crystals of HOF-11 were obtained by allowing hexane to slowly diffuse into a tetrahydrofuran solution of TCPA. It is also very easy to be regenerated using this method.

Crystal Structure of HOF-11. Single crystal X-ray diffraction investigation discloses that HOF-11 belongs to the monoclinic system with the $P2_1/n$ space group. In the crystal structure, there are four crystallographic independent TCPA molecules in the asymmetric unit, Figure S1. Their differences have been clearly recognized by the different dihedral angles between the neighboring benzene rings in a range of 49.36–82.45°. The carboxylate···carboxylate dimer synthons connect the adjacent TCPA ligands together to give a 3D supramolecular network, Figure 1a,b. The distances of D···A in the carboxylate···carboxylate hydrogen-bonding dimers range from 2.582 to 2.637 Å, Table 2. Eleven 3D networks are interpenetrated to form the robust HOF-11, Figure 1c. Despite many such interpenetrated networks in HOF-11, there are still one-dimensional (1D) channels in this HOF with the aperture size of 6.2 × 6.8 Å^2 along the [010] direction. The solvent molecules are filled in the channels, and the calculated solvent-accessible space is 33.2%. Topologically, TCPA is able to be regarded as a three-connected node (Figure 1d), and the sole 3D supramolecular network can be simplified as a (10,3)-b topology (Figure 1e,f).

The bulk material of as-synthesized HOF-11 was investigated using PXRD analysis (Figure S2), confirming the purity. The PXRD of HOF-11 after the treatment at the temperatures at 70 to 140 °C are very consistent with that of as-synthesized species, illustrating the robust nature and thermal stability in this temperature range. The PXRD pattern of HOF treated at 210 °C shows obvious change in comparison with that of as-synthesized phase, indicating the HOF framework being thermally unstable at this temperature. In addition, after the immersion of this HOF in water, the PXRD pattern of treated sample reveals that HOF-11 is very stable in water, Figure S3. The solvent molecules of this HOF were gradually removed (obsd. 14.0%) in the temperature range from 25 to 220 °C. The organic component begins to decompose at 290 °C, Figure S4.

Establishment of Permanent Porosity of HOF-11a. In the crystallization process, no high-boiling-point solvents were used, and thus as-synthesized HOF-11 was directly degassed at room temperature under high vacuum for 24 h to remove the solvent molecules located in the cavities. As shown in Figure S5, the PXRD pattern of activated framework (HOF-11a) still retains crystalline, which is very consistent with that of the as-synthesized phase, illustrating the robust nature. Nevertheless, the single structure of HOF-11a still is able to be resolved by single crystal X-ray diffraction analysis, the crystallographic data, as well as the hydrogen-bonding geometry of HOF-11a crystal being similar to that of as-prepared HOF-11, further demonstrating the robustness of this HOF, Tables 1 and 2. The TGA curve of HOF-11a reveals that there are not any residual solvent molecules in HOF-11a, Figure S4. The activated sample was employed to investigate the permanent porosity. However, there is not a N_2 adsorption at 77 K,

Table 2. Hydrogen Bonding Interactions of HOF-11 and HOF-11a[a]

D−H···A	distance of H···A (Å)	distance of D···A (Å)	angle of D−H···A (deg)
O2−H2A···O13#1	1.792/1.818	2.615/2.649	166.10/170.09
O16−H16A···O20#1	1.795/1.801	2.634/2.639	175.96/175.33
O14−H14···O1#2	1.775/1.768	2.598/2.594	166.00/167.33
O19−H19A···O15#2	1.766/1.789	2.604/2.6228	175.60/176.94
O4−H4···O3#3	1.802/1.808	2.637/2.643	173.02/172.50
O6−H6A···O17#4	1.754/1.771	2.582/2.589	168.35/163.92
O21−H21···O9#5	1.801/1.836	2.629/2.664	168.28/168.50
O10−H10A···O22#6	1.765/1.785	2.591/2.612	167.13/167.90
O18−H18···O5#7	1.804/1.825	2.624/2.639	164.78/163.04
O8−H8A···O24#8	1.803/1.826	2.627/2.650	166.40/166.51
O23−H23A···O7#9	1.773/1.782	2.596/2.605	165.99/165.87
O11−H11A···O12#10	1.787/1.787	2.606/2.627	164.30/178.64

[a]Symmetric code, #1: $x+1, y, z$, #2: $x-1, y, z$, #3: $-x-1, -y, -z+1$, #4: $x+3/2, -y+1/2, z+1/2$, #5: x+3/2, $-y+3/2, z-1/2$, #6: $x-3/2, -y+3/2, z+1/2$, #7: $x-3/2, -y+1/2, z-1/2$, #8: $x-2, y, z$, #9: $x+2, y, z$, #10: $-x+2, -y+1, -z+1$.

DOI: 10.1021/acs.cgd.7b01322
Cryst. Growth Des. XXXX, XXX, XXX−XXX

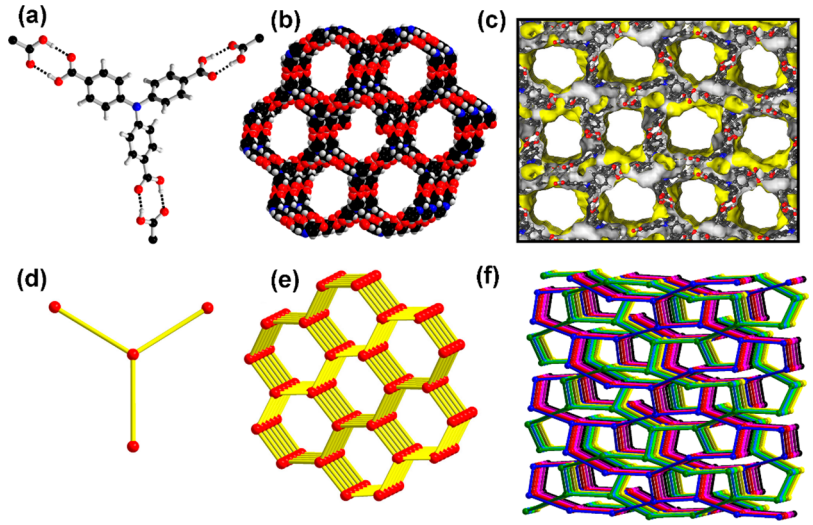

Figure 1. Crystal structures of HOF-11 showing (a) a TCPA molecule and hydrogen bonding interactions between neighboring carboxylate groups from different TCPA modules (carbon: black; hydrogen: white; nitrogen: blue); (b) a three-dimensional (3D) hydrogen-bonded supramolecular network; (c) packing diagrams of HOF-11 along the [010] direction; (d) a TCPA molecule was regarded as a 3-connected node; (e) a (10,3)-b topology; and (f) a 3D interpenetrated topological networks along the [010] direction (different colors represent different networks).

because the gas diffusion has been prevented in the channel of HOF due to the strong interactions between nitrogen and the pore window.[18,25] Such phenomena are very common for HOFs.[13,14,18,25−29] The typical type-I CO_2 adsorption isotherm at 196 K clearly reveals the microporous nature of HOF-11a, Figure 2. The Brunauer−Emmett−Teller (BET) surface area is

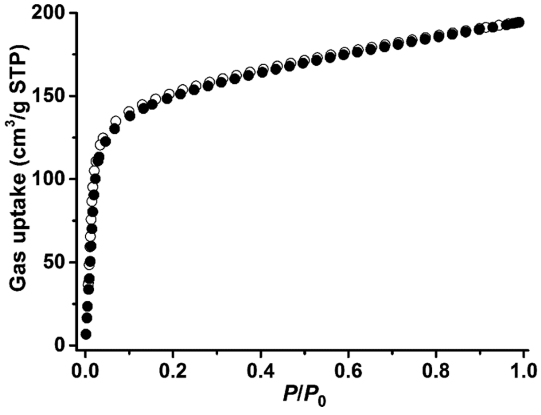

Figure 2. CO_2 sorption isotherm of activated HOF-11a at 196 K (solid symbols: adsorption, open symbols: desorption).

deduced to be 687 m^2/g. CO_2 uptake is ~194 cm^3/g at 196 K and 1 atm, and the experimental pore volume of HOF-11a was calculated as 0.35 cm^3/g, which is almost matched with the theoretical value, 0.33 cm^3/g, on the basis of the crystal structure of HOF-11a.

Gas Sorption of HOF-11a. Given the fact that the gas separations at ambient temperatures have been hot topics with potential use in practice,[49,50] a series of single component, including C_2H_2, CO_2, CH_4, and N_2, sorption isotherms of HOF-11a have been collected at 273 and 298 K. As can be seen in Figure 3, HOF-11a was found to absorb C_2H_2 (45 cm^3/g), CO_2 (30 cm^3/g), CH_4 (8 cm^3/g), and N_2 (2 cm^3/g) at 1 atm and 296 K. Following the temperature being lowered to 273 K, the uptakes of C_2H_2, CO_2, CH_4, and N_2 were increased to 74, 49, 13, and 4 cm^3/g, respectively. The C_2H_2 and CO_2 uptakes

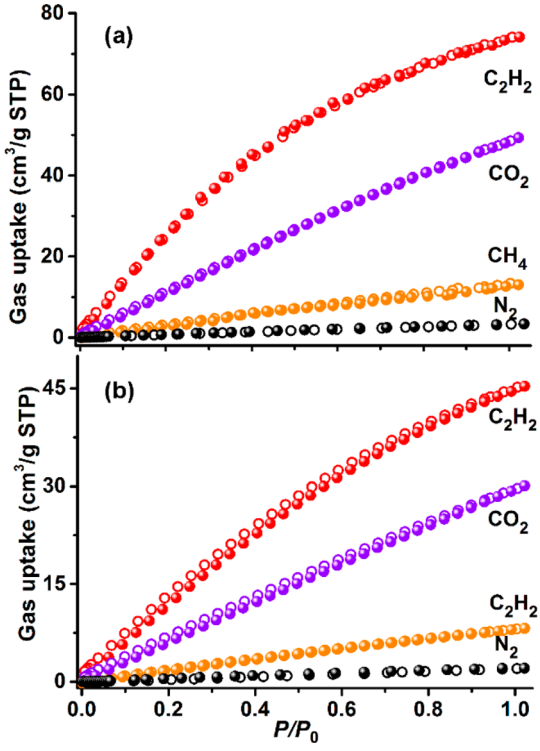

Figure 3. C_2H_2, CO_2, CH_4, and N_2 sorption isotherms of HOF-11a at 273 K (a) and 296 K (b) (C_2H_2: red, CO_2: violet, CH_4: orange, N_2: black, solid symbols: adsorption, open symbols: desorption).

are comparable with some MOFs, such as SNNU-80,[51] UPC-8,[52] $[Co_3(\mu\text{-}OH)(NPy_3)(bpdc)_3]$,[53] at the same conditions. According to the virial method, the coverage-dependent adsorption enthalpies of HOF-11a toward C_2H_2, CO_2, CH_4, and N_2 have been calculated, revealing the enthalpies at zero coverage: 22, 21, 16, and 12 kJ/mol, respectively. The enthalpy values of C_2H_2 and CO_2 at zero coverage are very consistent with that of reported HOFs,[13,29] manifesting the presence of moderately strong interactions between the C_2H_2/CO_2

DOI: 10.1021/acs.cgd.7b01322
Cryst. Growth Des. XXXX, XXX, XXX−XXX

molecules and HOF-11a. The different interactions between gases and HOF-11a are helpful to differentiate these molecules.

The obviously different uptakes and affinities of HOF-11a toward these different gases due to the molecular size and polarity imply the potential application of HOF-11a for the industrial separations of C_2H_2/CH_4, CO_2/CH_4, and CO_2/N_2. The selectivity of C_2H_2/CH_4 (50%:50%), CO_2/CH_4 (50%:50%), and CO_2/N_2 (15%:85%) mixture was explored by virtue of the popular ideal adsorbed solution theory (IAST) method. As shown in Figure 4, the predicted gas adsorption

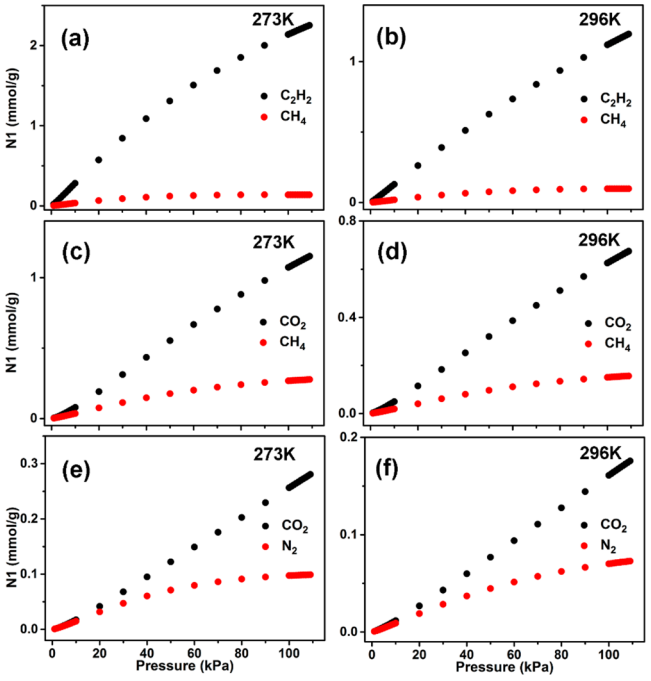

Figure 4. (a–f) Mixture adsorption isotherms predicted by IAST of HOF-11a for C_2H_2/CH_4 (C_2H_2/CH_4 = 50%:50%), CO_2/CH_4 (CO_2/CH_4 = 50%:50%), and CO_2/N_2 (15%:85%) at 273 and 296 K.

isotherms based on IAST method are closely dependent on the pressure and temperature. The C_2H_2/CH_4, CO_2/CH_4 and CO_2/N_2 molar selectivity were determined to be 11.6, 4.2, and 13.1, respectively, at 296 K under 1 atm. With the temperature being decreased to 273 K, all C_2H_2/CH_4, CO_2/CH_4, and CO_2/N_2 selectivity values are 15.5, 4.0, and 15.1, respectively. The theoretical C_2H_2/CH_4 and CO_2/CH_4 molar selectivity for HOF-11a are ~12 and 4, respectively, at 273 K under 1 atm, which are slightly smaller than those HOFs with excellent separation performance, such as SOF-1a[13] (34 and 6 estimated by Henry's constants) and HOF-5a[29] (-- and 6). The CO_2/N_2 selectivity for a 10:90 mixture is 15.1 at 296 K and 1 atm, which is even comparable with zeolitic imidazolate frameworks like ZIF-9S[54] (18), underlying the capability in postcombustion CO_2 capture.

CONCLUSIONS

In summary, we have successfully realized a robust 3D microporous hydrogen-bonded organic framework with a 11-fold interpenetrated structure. The permanent porosity of the desolvated framework was well established by means of CO_2 sorption, showing a moderately high BET surface area of 687 m^2/g. This microporous HOF exhibits selective capture of C_2H_2 and CO_2 over CH_4 and N_2 and shows a potential gas separation capability, as clearly demonstrated by the experimental results and theoretical IAST calculations. This work indicates the power of -COOH groups for the assembly of porous HOFs. Given the fact that -COOH is one of the richest groups for numerous organic linkers, this work will facilitate extensive research on the design and construction of multifunctional HOFs based on -COOH moieties. Furthermore, different combination modes between various organic skeletons and hydrogen-bonding moieties can provide versatile HOFs with different structures and properties. We are now developing new building blocks for robust HOFs with diverse applications.

ASSOCIATED CONTENT

Supporting Information

The Supporting Information is available free of charge on the ACS Publications website at DOI: 10.1021/acs.cgd.7b01322.

Crystal structures of four kinds of TPCA ligands and powder X-ray diffraction patterns (PDF)

Accession Codes

CCDC 1573633–1573634 contain the supplementary crystallographic data for this paper. These data can be obtained free of charge via www.ccdc.cam.ac.uk/data_request/cif, or by emailing data_request@ccdc.cam.ac.uk, or by contacting The Cambridge Crystallographic Data Centre, 12 Union Road, Cambridge CB2 1EZ, UK; fax: +44 1223 336033.

AUTHOR INFORMATION

Corresponding Authors

*E-mail: hailong.wang@utsa.edu (H.W.).
*E-mail: banglin.chen@utsa.edu (B.C.).

ORCID

Banglin Chen: 0000-0001-8707-8115

Notes

The authors declare no competing financial interest.

ACKNOWLEDGMENTS

This work was supported by the NSF Award DMR-1606826 and Welch Foundation Grant AX-1730 (B.C.) and AX-1593 (J.C.G.Z.). We thank Prof. Dr. Shengqian Ma and Dr. Zheng Niu for the helpful discussion on the crystal structure determination.

REFERENCES

(1) Barrer, R. M.; Shanson, V. H. *J. Chem. Soc., Chem. Commun.* **1976**, 333.
(2) Hasell, T.; Cooper, A. I. *Nat. Rev. Mater.* **2016**, *1*, 16053.
(3) Sun, J.-K.; Zhan, W.-W.; Akita, T.; Xu, Q. *J. Am. Chem. Soc.* **2015**, *137*, 7063.
(4) Cooper, A. I. *ACS Cent. Sci.* **2017**, *3*, 544.
(5) Tian, J.; Thallapally, P. K.; McGrail, B. P. *CrystEngComm* **2012**, *14*, 1909.
(6) McKeown, N. B. *J. Mater. Chem.* **2010**, *20*, 10588.
(7) Mastalerz, M. *Chem. - Eur. J.* **2012**, *18*, 10082.
(8) Sozzani, P.; Bracco, S.; Comotti, A.; Ferretti, L.; Simonutti, R. *Angew. Chem., Int. Ed.* **2005**, *44*, 1816.
(9) Liu, Y.; Hu, C.; Comotti, A.; Ward, M. D. *Science* **2011**, *333*, 436.
(10) Simard, M.; Wuest, J. D.; Su, D. *J. Am. Chem. Soc.* **1991**, *113*, 4696.
(11) Wuest, J. D. *Chem. Commun.* **2005**, 5830.
(12) Adachi, T.; Ward, M. D. *Acc. Chem. Res.* **2016**, *49*, 2669.
(13) Yang, W.; Greenaway, A.; Lin, X.; Matsuda, R.; Blake, A. J.; Wilson, C.; Lewis, W.; Hubberstey, P.; Kitagawa, S.; Champness, N. R.; Schröder, M. J. *J. Am. Chem. Soc.* **2010**, *132*, 14457.

DOI: 10.1021/acs.cgd.7b01322
Cryst. Growth Des. XXXX, XXX, XXX–XXX

(14) He, Y.; Xiang, S.; Chen, B. *J. Am. Chem. Soc.* **2011**, *133*, 14570.
(15) Pulido, A.; Chen, L.; Kaczorowski, T.; Holden, D.; Little, M. A.; Chong, S. Y.; Slater, B. J.; McMahon, D. P.; Bonillo, B.; Stackhouse, C. J.; Stephenson, A.; Kane, C. M.; Clowes, R.; Hasell, T.; Cooper, A. I.; Day, G. M. *Nature* **2017**, *543*, 657.
(16) Hu, F.; Liu, C.; Wu, M.; Pang, J.; Jiang, F.; Yuan, D.; Hong, M. *Angew. Chem., Int. Ed.* **2017**, *56*, 2101.
(17) Mastalerz, M.; Oppel, I. M. *Angew. Chem., Int. Ed.* **2012**, *51*, 5252.
(18) Nugent, P. S.; Rhodus, V. L.; Pham, T.; Forrest, K.; Wojtas, L.; Space, B.; Zaworotko, M. J. *J. Am. Chem. Soc.* **2013**, *135*, 10950.
(19) Yan, W.; Yu, X.; Yan, T.; Wu, D.; Ning, E.; Qi, Y.; Han, Y.-F.; Li, Q. *Chem. Commun.* **2017**, *53*, 3677.
(20) Lin, Y.; Jiang, X.; Kim, S. T.; Alahakoon, S. B.; Hou, X.; Zhang, Z.; Thompson, C. M.; Smaldone, R. A.; Ke, C. *J. Am. Chem. Soc.* **2017**, *139*, 7172.
(21) Ju, Z.; Liu, G.; Chen, Y.-S.; Yuan, D.; Chen, B. *Chem. - Eur. J.* **2017**, *23*, 4774.
(22) Lü, J.; Perez-Krap, C.; Suyetin, M.; Alsmail, N. H.; Yan, Y.; Yang, S.; Lewis, W.; Bichoutskaia, E.; Tang, C. C.; Blake, A. J.; Cao, R.; Schröder, M. *J. Am. Chem. Soc.* **2014**, *136*, 12828.
(23) Luo, X.-Z.; Jia, X.-J.; Deng, J.-H.; Zhong, J.-L.; Liu, H.-J.; Wang, K.-J.; Zhong, D.-C. *J. Am. Chem. Soc.* **2013**, *135*, 11684.
(24) Chen, T.-H.; Popov, I.; Kaveevivitchai, W.; Chuang, Y.-C.; Chen, Y.-S.; Daugulis, O.; Jacobson, A. J.; Miljanić, O. Š. *Nat. Commun.* **2014**, *5*, 5131.
(25) Wang, H.; Wu, H.; Kan, J.; Chang, G.; Yao, Z.; Li, B.; Zhou, W.; Xiang, S.; Zhao, J. C.-G.; Chen, B. *J. Mater. Chem. A* **2017**, *5*, 8292.
(26) Zhou, D.-D.; Xu, Y.-T.; Lin, R.-B.; Mo, Z.-W.; Zhang, W.-X.; Zhang, J.-P. *Chem. Commun.* **2016**, *52*, 4991.
(27) Li, P.; He, Y.; Guang, J.; Weng, L.; Zhao, J. C.-G.; Xiang, S.; Chen, B. *J. Am. Chem. Soc.* **2014**, *136*, 547.
(28) Li, P.; He, Y.; Arman, H. D.; Krishna, R.; Wang, H.; Weng, L.; Chen, B. *Chem. Commun.* **2014**, *50*, 13081.
(29) Wang, H.; Li, B.; Wu, H.; Hu, T.-L.; Yao, Z.; Zhou, W.; Xiang, S.; Chen, B. *J. Am. Chem. Soc.* **2015**, *137*, 9963.
(30) Wang, H.; Bao, Z.; Wu, H.; Lin, R.-B.; Zhou, W.; Hu, T.-L.; Li, B.; Zhao, J. C.-G.; Chen, B. *Chem. Commun.* **2017**, *53*, 11150.
(31) Dalapati, S.; Saha, R.; Jana, S.; Patra, A. K.; Bhaumik, A.; Kumar, S.; Guchhait, N. *Angew. Chem., Int. Ed.* **2012**, *51*, 12534.
(32) Karmakar, A.; Illathvalappil, R.; Anothumakkool, B.; Sen, A.; Samanta, P.; Desai, A. V.; Kurungot, S.; Ghosh, S. K. *Angew. Chem., Int. Ed.* **2016**, *55*, 10667.
(33) Yang, W.; Yang, F.; Hu, T.-L.; King, S. C.; Wang, H.; Wu, H.; Zhou, W.; Li, J.-R.; Arman, H. D.; Chen, B. *Cryst. Growth Des.* **2016**, *16*, 5831.
(34) Li, P.; He, Y.; Zhao, Y.; Weng, L.; Wang, H.; Krishna, R.; Wu, H.; Zhou, W.; O'Keeffe, M.; Han, Y.; Chen, B. *Angew. Chem., Int. Ed.* **2015**, *54*, 574.
(35) Dalrymple, S. A.; Shimizu, G. K. H. J. *J. Am. Chem. Soc.* **2007**, *129*, 12114.
(36) Zentner, C. A.; Lai, H. W. H.; Greenfield, J. T.; Wiscons, R. A.; Zeller, M.; Campana, C. F.; Talu, O.; FitzGerald, S. A.; Rowsell, J. L. C. *Chem. Commun.* **2015**, *51*, 11642.
(37) Hisaki, I.; Nakagawa, S.; Ikenaka, N.; Imamura, Y.; Katouda, M.; Tashiro, M.; Tsuchida, H.; Ogoshi, T.; Sato, H.; Tohnai, N.; Miyata, M. *J. Am. Chem. Soc.* **2016**, *138*, 6617.
(38) Xiao, W.; Hu, C.; Ward, M. D. *J. Am. Chem. Soc.* **2014**, *136*, 14200.
(39) Kolotuchin, S. V.; Fenlon, E. E.; Wilson, S. R.; Loweth, C. J.; Zimmerman, S. C. *Angew. Chem., Int. Ed. Engl.* **1996**, *34*, 2654.
(40) Bajpai, A.; Venugopalan, P.; Moorthy, J. N. *Cryst. Growth Des.* **2013**, *13*, 4721.
(41) Lai, H. W. H.; Wiscons, R. A.; Zentner, C. A.; Zeller, M.; Rowsell, J. L. C. *Cryst. Growth Des.* **2016**, *16*, 821.
(42) Cremer, J.; Bäuerle, P. *J. Mater. Chem.* **2006**, *16*, 874.
(43) Nandi, S.; Chakraborty, D.; Vaidhyanathan, R. *Chem. Commun.* **2016**, *52*, 7249.
(44) Sheldrick, G. M. *Acta Crystallogr., Sect. A: Found. Crystallogr.* **2008**, *64*, 112.
(45) Spek, A. L. *PLATON, A Multipurpose Crystallographic Tool*; Utrecht University: Utrecht, the Netherlands, 2005.
(46) Li, B.; Zhang, Y.; Krishna, R.; Yao, K.; Han, Y.; Wu, Z.; Ma, D.; Shi, Z.; Pham, T.; Space, B.; Liu, J.; Thallapally, P. K.; Liu, J.; Chrzanowski, M.; Ma, S. *J. Am. Chem. Soc.* **2014**, *136*, 8654.
(47) Banerjee, D.; Zhang, Z.; Plonka, A. M.; Li, J.; Parise, J. B. *Cryst. Growth Des.* **2012**, *12*, 2162.
(48) Myers, A. L.; Prausnitz, J. M. *AIChE J.* **1965**, *11*, 121.
(49) Bao, Z.; Chang, G.; Xing, H.; Krishna, R.; Ren, Q.; Chen, B. *Energy Environ. Sci.* **2016**, *9*, 3612.
(50) Chen, B.; Xiang, S.; Qian, G. *Acc. Chem. Res.* **2010**, *43*, 1115.
(51) Hou, X.-Y.; Wang, X.; Li, S.-N.; Jiang, Y.-C.; Hu, M.-C.; Zhai, Q.-G. *Cryst. Growth Des.* **2017**, *17*, 3229.
(52) Xiao, Z.; Wang, Y.; Zhang, S.; Fan, W.; Xin, X.; Pan, X.; Zhang, L.; Sun, D. *Cryst. Growth Des.* **2017**, *17*, 4084.
(53) Hua, C.; Yang, Q.-Y.; Zaworotko, M. J. *Cryst. Growth Des.* **2017**, *17*, 3475.
(54) Wang, B.; Côté, A. P.; Furukawa, H.; O'Keeffe, M.; Yaghi, O. M. *Nature* **2008**, *453*, 207.

DOI: 10.1021/acs.cgd.7b01322
Cryst. Growth Des. XXXX, XXX, XXX−XXX